Behavioral/Systems/Cognitive

The Projective Field of a Retinal Amacrine Cell

Saskia E. J. de Vries,[1,2] **Stephen A. Baccus,**[1] **and Markus Meister**[1,2]

[1]Department of Molecular and Cellular Biology and Center for Brain Science and [2]Program in Neurosciences, Harvard University, Cambridge, Massachusetts 02138

In sensory systems, neurons are generally characterized by their receptive field, namely the sensitivity to activity patterns at the input of the circuit. To assess the role of the neuron in the system, one must also know its projective field, namely the spatiotemporal effects the neuron exerts on all of the outputs of the circuit. We studied both the receptive and projective fields of an amacrine interneuron in the salamander retina. This amacrine type has a sustained OFF response with a small receptive field, but its output projects over a much larger region. Unlike other amacrine cells, this type is remarkably promiscuous and affects nearly every ganglion cell within reach of its dendrites. Its activity modulates the sensitivity of visual responses in ganglion cells but leaves their kinetics unchanged. The projective field displays a center-surround structure: depolarizing a single amacrine suppresses the visual sensitivity of ganglion cells nearby and enhances it at greater distances. This change in sign is seen even within the receptive field of one ganglion cell; thus, the modulation occurs presynaptically on bipolar cell terminals, most likely via GABA$_B$ receptors. Such an antagonistic projective field could contribute to the mechanisms of the retina for predictive coding.

Introduction

The retina is an intricate neural circuit that processes the raw visual image created by the optics of the eye and conveys the results to the brain via parallel populations of retinal ganglion cells (Wässle, 2004; Segev et al., 2006; Baccus, 2007; Field and Chichilnisky, 2007; Gollisch and Meister, 2010). There is great interest in how these visual computations are implemented in synaptic circuits of the retina. Interposed between photoreceptors and ganglion cells (GCs) is a wide diversity of interneurons, perhaps 50 types in all (Masland, 2001). To assign a functional role to each of these interneurons, one must know how the neuron is influenced by the input layer of photoreceptors and how its activity propagates to the output layer of ganglion cells. To answer the first question, one traditionally stimulates the receptors and monitors the response of the interneuron, leading to a measurement of its receptive field; this is perhaps the most common activity in sensory neuroscience. For the second question, one could stimulate the interneuron and monitor the resulting effects among all the output neurons, which collectively can be termed the "projective field." Although knowing this complement to the receptive field has long been recognized as essential (Lehky and Sejnowski, 1988), it is studied only rarely.

The most mysterious retinal neurons are the amacrine cells. These inhibitory interneurons provide the majority of synaptic input to ganglion cells (Wässle and Boycott, 1991; Jacoby et al., 1996; Masland, 1999; Pang et al., 2002) and exert inhibition at the axon terminal of bipolar cells (Tachibana and Kaneko, 1988; Dong and Werblin, 1998). Thus, they shape and control the signals that ganglion cells receive from the outer retina. Amacrine cells in general are credited with contributing to the antagonistic surround of ganglion cell receptive fields (Cook and McReynolds, 1998; Taylor, 1999; Flores-Herr et al., 2001), making light responses more transient (Nirenberg and Meister, 1997; Dong and Werblin, 1998; Roska et al., 1998), implementing direction-selective processing (Zhou and Lee, 2008), and conveying long-range signals far across the retina (Werblin and Copenhagen, 1974; Olveczky et al., 2003). It is thought that each of the ~30 amacrine types has a distinct role in the retina (Masland, 1999), yet the correspondence is known in only a few instances, such as the AII cell (Masland, 1999; Münch et al., 2009), starburst cells (He and Masland, 1997; Euler et al., 2002), and certain wide-field amacrine cells (Baccus et al., 2008). Under these conditions, it is essential to survey the amacrine cell class further and delineate their possible functions.

In the present study, we focus on an amacrine type with a distinctive "sustained OFF" light response (Zhang and Wu, 2010). We controlled single amacrine cells with an intracellular microelectrode, while stimulating the photoreceptor layer with light and simultaneously recording from the population of ganglion cells using a multielectrode array. This novel approach yielded both the receptive and the projective fields of the amacrine cell and revealed its role in the flow of retinal information.

Materials and Methods

Recording. The retina of a larval tiger salamander (of either sex) was isolated and bathed in oxygenated Ringer's solution at room temperature. It was placed on a multielectrode array, ganglion cell layer facing down, and held in place by a dialysis membrane covered with a thin layer of 0.5% agarose (type III-A: High EEO; Sigma). The multielectrode array consisted of 61 platinized electrodes arranged at 60 μm spacing in a hexag-

onal grid 500 μm across. The array recorded spike trains from many ganglion cells simultaneously, sampling ~15% of the population (Meister et al., 1994). To record intracellularly from amacrine cells, a sharp microelectrode, filled with 2 M potassium acetate and 3% rhodamine dextran (10,000 molecular weight; Invitrogen) at a final impedance of 150–250 MΩ, was passed through a hole in the dialysis membrane and the layer of agarose. After recording, some of the cells were filled iontophoretically (1–5 nA pulses, 5–10 min) fixed in 4% paraformaldehyde and imaged using a confocal microscope with a 40× oil-immersion objective.

Pharmacological agents that interfere with synaptic transmission were added to the superfusate as described in text and legends. For block of GABA$_B$ transmission, we chose the agonist baclofen, because the common antagonists, including phaclofen and saclofen, are not effective in the salamander retina (Tian and Slaughter, 1994). Experiments with the antagonist CGP 35348 (3-Aminopropyl)(diethoxymethyl) phosphoric acid were inconclusive.

In all, the reported results are based on recordings from 15 sustained OFF amacrine cells (SOAs) and 218 ganglion cells.

Stimulation. Visual stimuli were projected from a computer monitor onto the photoreceptor layer of the retina, at a photopic mean intensity of ~8 mW/m^2, equivalent to 11,000 photons/μm^2/s at 630 nm for the salamander's red cone. Periodic flash stimuli were spatially uniform white light, flashing on and off at 0.5 Hz. Linear–nonlinear (LN) models were calculated from responses to a spatially uniform flickering white light (Baccus and Meister, 2002), whose intensity was changed every 30 ms based on a Gaussian probability distribution with contrast (SD/mean) of 0.20. The spatial receptive fields of all neurons were measured by reverse correlation to a flickering black and white checkerboard stimulus (Baccus et al., 2008). The profile of the reverse correlation function was fit with a two-dimensional paraboloid. The receptive field radius is quoted as the geometric average of the two half axes of the ellipse at the base of the paraboloid.

LN model. To characterize temporal processing of a uniform light stimulus, we used an LN model to fit the response of each ganglion cell to the uniform flicker stimulus (Chichilnisky, 2001; Baccus and Meister, 2002). The model parameters consist of a linear temporal filter and an instantaneous nonlinearity. The predicted response of the cell, $r'(t)$, is computed by convolving the stimulus $s(t)$ with the linear filter $F(\tau)$ and passing the result, $g(t)$, through the nonlinearity $N(g)$:

$$r'(t) = N(\int s(t - \tau) F(\tau) d\tau). \qquad (1)$$

Within this approximation, the linear filter represents the temporal sensitivity of the cell, whereas the nonlinearity conveys the threshold, gain, and rectification of the response of the cell. The optimal values for linear filter and nonlinearity were computed as described (Baccus and Meister, 2002).

Amacrine circuit model. In the direct pathway of Figure 7, the stimulus $s(t)$ was first convolved with a monophasic filter $F_B(\tau)$ taken to represent processing in the outer retina. This was followed by a bi-
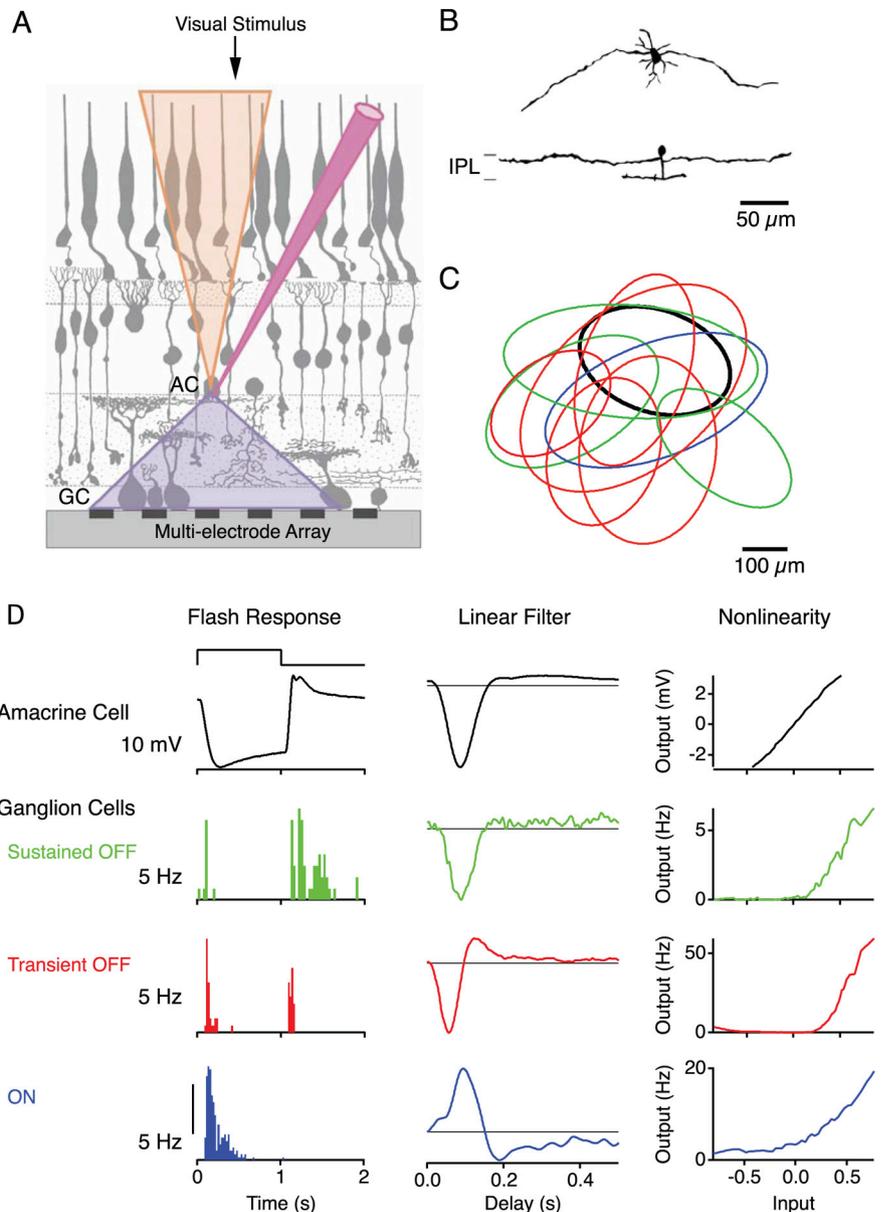
Figure 1. Experimental approach. **A**, Schematic of recording technique. A single amacrine cell (AC) is impaled with a sharp electrode, while a population of GCs are recorded using a multielectrode array. The receptive field of the amacrine cell (top cone) represents the convergence of signals from photoreceptors, whereas the projective field of the cell (bottom cone) specifies the divergence of its output onto ganglion cells. **B**, Tangential (top) and vertical (bottom) views of two different sustained OFF amacrine cells, obtained from confocal micrographs. IPL, Inner plexiform layer. **C**, The receptive field centers of a sustained OFF amacrine cell (bold line) and several ganglion cells of different types (thin lines; see **D** for color legend) recorded in a sample experiment. Each outline represents the base of a paraboloid fit to the receptive field profile (see Materials and Methods). **D**, Visual responses of representative cells from **C**. Left, Responses to a 1 s step of light (top trace), averaged over 15 repeats; membrane potential for the AC, and firing rate for the GCs. Middle and Right, The linear filter and the nonlinearity of the linear–nonlinear model derived from responses to spatially uniform random flicker.

phasic filter $F_D(\tau)$ that represents high-pass processing in the inner retina. Its impulse response was chosen as a differentiating function with a peak at 25 ms to constrain an overall solution to the model. Then, $F_B(\tau)$ was computed so as to yield an overall ganglion cell temporal filter equivalent to the measured linear filter of the ganglion cell LN model (supplemental Fig. S3A, available at www.jneurosci.org as supplemental material). The output of the two filters was then passed through an instantaneous nonlinearity $N(z)$, taken again from the LN model of the response of the ganglion cell. In the amacrine pathway, the visual response of the amacrine cell was modeled as an LN cascade with filter $F_A(\tau)$ followed by nonlinearity $N_A(q)$, both
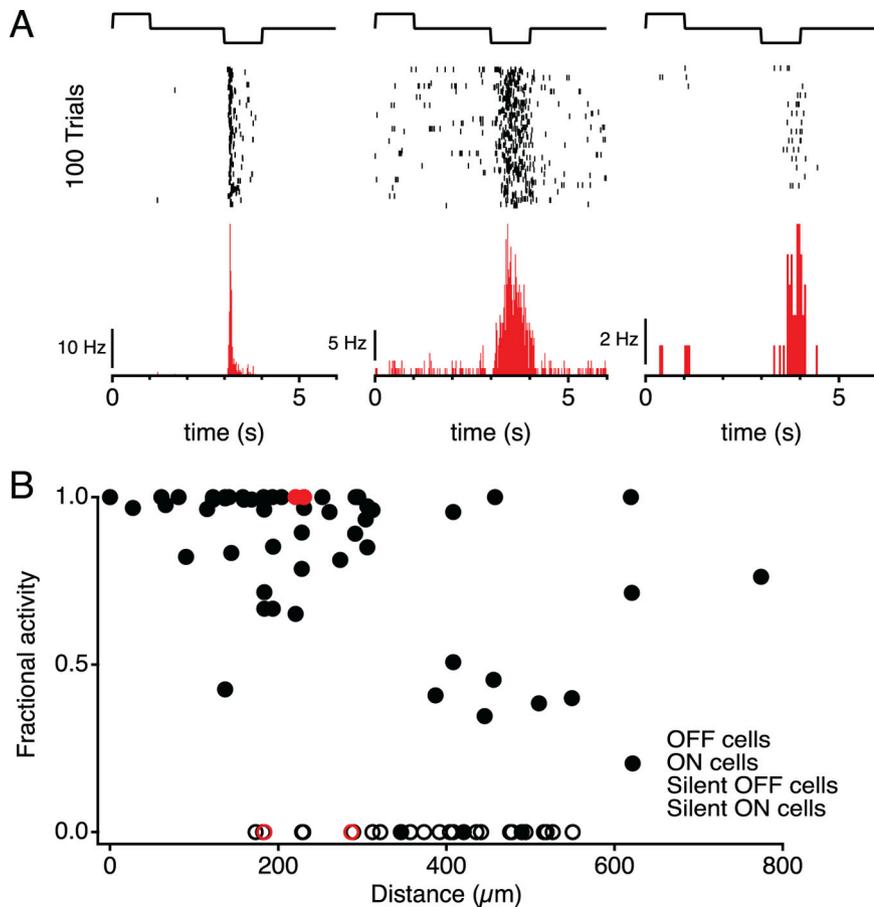
Figure 2. Hyperpolarization of a single sustained OFF amacrine cell disinhibits local ganglion cells. **A**, Spiking responses from a transient OFF (left), sustained OFF (middle), and ON (right) ganglion cell after current injection into a sustained OFF amacrine cell. Top, Current stimulus (±0.5 nA). Middle, Raster of spikes on 100 trials. Bottom, Average firing rate over trials. **B**, Disinhibition of ganglion cell firing plotted as a function of distance from the stimulated SOA. This is the fraction of the spikes of a ganglion cell that occurred during the 1 s hyperpolarizing current step in the experiment of **A**. "Silent" GCs did not fire during this procedure but were active during light stimulation. Based on recordings of eight SOAs and 87 GCs.

derived from a fit to the light response of the SOA. Synaptic transmission from the amacrine cell was modeled with an instantaneous sigmoidal gain function $G(u)$, followed by a filter $F_S(\tau)$ that represents the delay in slow GABA$_B$ processing. This delay filter was computed so as to fit the ganglion cell firing rate resulting from a current pulse injected into the amacrine cell (see Fig. 2A) (supplemental Fig. S3B, available at www.jneurosci.org as supplemental material). The amplitude of the inhibitory gain function was set so that the maximal effect of the amacrine pathway was to reduce the gain of the direct pathway by a factor of two. Mathematically, the response of the model is given by the following equations (see Fig 7A):

$$r'(t) = N(z(t))$$

$$z(t) = \int y(t - \tau) F_D(\tau) d\tau$$

$$y(t) = x(t) \cdot w(t)$$

$$x(t) = \int s(t - \tau) F_B(\tau) d\tau$$

$$w(t) = \int v(t - \tau) F_S(\tau) d\tau \qquad (2)$$

$$v(t) = G(u(t))$$

$$u(t) = N_A(q(t))$$

$$q(t) = \int s(t - \tau) F_A(\tau) d\tau.$$

Results

An amacrine cell with sustained OFF light response

To examine the projective field of retinal interneurons, we recorded simultaneously from a single interneuron and a population of GCs. This arrangement (Fig. 1A) allowed us to examine the visual response properties of both the interneuron and the GCs and to explore their functional connections. In the initial studies, we examined many different amacrine cells that exhibited diverse response properties. Among these, we found a subset that had a strong direct effect on ganglion cells. These amacrine cells all produced a sustained hyperpolarization in response to a step of light (Zhang and Wu, 2010), lasting for the duration of the stimulus (Fig. 1D, top row). Based on this light response, we refer to them as sustained OFF amacrine cells (SOAs).

The SOAs typically had a dendritic field of ~100 μm radius (Fig. 1B). In some cells, the dendritic arbor included two large processes emerging from the soma in opposite directions, whereas other cells had multiple small processes. The receptive field of the SOA extended somewhat beyond the dendritic field: the radius of the receptive field center was measured at 132 ± 24 μm (mean ± SD) (Fig. 1C).

Our grouping of the sustained OFF amacrine cells was based entirely on their function, namely the similarities of their receptive fields and the uniformity of their effects on downstream ganglion cells. They accounted for ~45% of our sharp electrode recordings from confirmed amacrine cells, but this only serves as an upper bound on their prevalence, because many neurons of the inner nuclear layer with other response properties were not fully characterized. It is possible that this cell type encompasses neurons that can be further separated by other physiological or morphological criteria, yet, given the consistent effects of these amacrine cells, we discuss them here as a single type.

In a similar manner, we classified GCs by their visual responses. In addition to the traditional periodic light flashes, we used a random flicker stimulus and an LN model to capture the visual responses of the cells (see Materials and Methods). In this model, the visual stimulus is convolved with a linear temporal filter and the result is passed through an instantaneous nonlinearity to yield the predicted response of the cell (Chichilnisky, 2001). The linear filter reflects the average temporal filtering of the cell, and the nonlinearity captures the threshold, sensitivity, and saturation in the firing behavior of the GC. Examining the linear filters, we classified three types of ganglion cell. "Transient OFF" GCs had a fast biphasic OFF filter; they responded briefly to square-wave light flashes at the offset and often also at the onset. "Sustained OFF" GCs had slow monophasic filters and responded in a more sustained manner to the offset of light. "ON" cells responded at the onset

of light (Fig. 1*D*) (supplemental Fig. S1*B*, available at www.jneurosci.org as supplemental material).

Sustained OFF amacrine cells affect nearby ganglion cells with varying kinetics

The simplest approach to determine the projective field of the amacrine cell is to inject current into that cell and test for direct responses among the ganglion cells. We injected steps of ±0.5 nA into the amacrine cell, which caused voltage changes on the order of the visual flash response (<30 mV) and thus within the physiological range of the cell. Hyperpolarization of an SOA drove spiking activity in a number of nearby GCs (Fig. 2*A*). Among those GCs were many different visual response types: both ON and OFF, transient and sustained. This suggests that, even in the absence of visual stimuli, the SOA exerts a strong tonic inhibition on nearby GCs, which is relieved when the amacrine cell is hyperpolarized. This effect was strongest in a region close to the amacrine cell: 85% of the GCs recorded within 320 μm distance fired significantly more when the SOA was hyperpolarized. Thus, whereas this amacrine cell type receives visual information within a limited radius of 130 μm, its influence expands to project over 300 μm (Fig. 2*B*).

We recorded few ON ganglion cells in this study, nine in total, reflecting the OFF bias of the salamander retina (Burkhardt et al., 1998; Segev et al., 2006). However, those neurons responded to amacrine cell hyperpolarization in the same way as nearby OFF cells (Fig. 2*B*). Our following analysis will be limited to the more numerous OFF ganglion cells, except when noted.

Although the SOA cell influenced all GC types, the effects varied not only in strength but also in their time course. During SOA hyperpolarization in the dark, some GCs produced a transient burst of firing that peaked ~150 ms after onset of the current pulse and returned to baseline within 400 ms (Fig. 2*A*, left). Other GCs fired in a sustained manner throughout the duration of the 1 s pulse (Fig. 2*A*, center). Generally, the kinetics of the response of a GC to SOA current injection matched the kinetics of its response to visual stimuli, although some GCs with a sustained response to SOA stimulation showed a transient flash response (Fig. 3*A*).

To examine these relationships more closely, we quantified the response kinetics to the two types of stimuli. As mentioned above, the shape of the linear filter of a ganglion cell captures the average temporal sensitivity of the cell. In a principal components analysis of these filters across all recorded OFF GCs, the first principal component accounted for 70% of the variance (supplemental Fig. S2, available at www.jneurosci.org as supplemental material). Indeed, the projection of the filter on
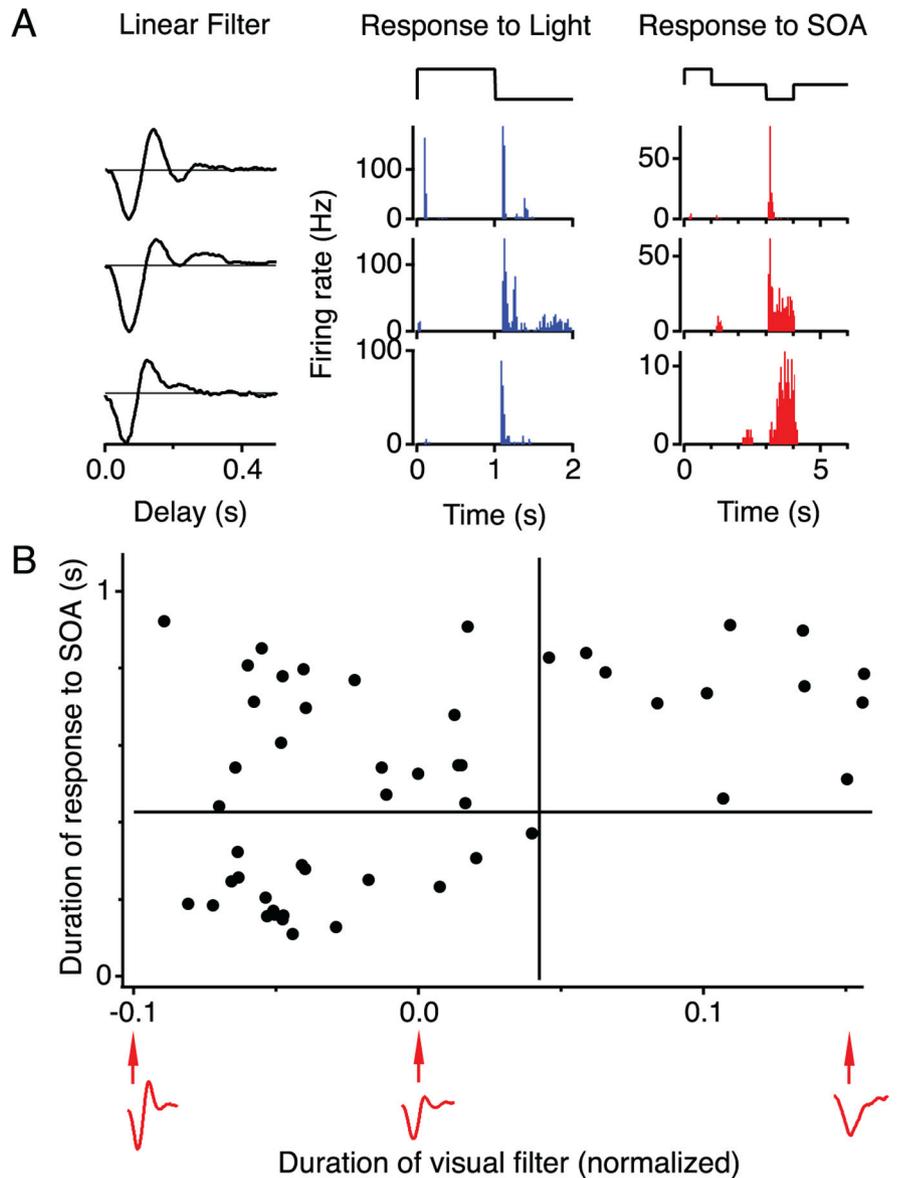
Figure 3. Visual stimulation and current injected in an SOA produce similar response kinetics in ganglion cells. *A*, Response of three sample ganglion cells to light and to current injection into an SOA. Left, Filter function of the LN model representing kinetics of the visual response of the GC. Middle, Firing rate during square-wave uniform light steps. Right, Firing rate during square-wave current injections (±0.5 nA) in the SOA. *B*, Duration of the response of a ganglion cell to SOA stimulation plotted against the duration of its visual response. Each point represents one GC. Ordinate shows the time required for the GC to fire 80% of the spikes in the burst after SOA hyperpolarization. Abscissa shows the projection of the linear filter of the GC onto the first principal component of the filter waveforms. Some sample filter shapes are provided below the axis. Note there are no GCs in the bottom right quadrant, representing cells with slow visual response but fast response to SOA stimulation. Based on recordings of eight SOAs and 50 GCs.

this component reliably distinguished fast biphasic from slow monophasic filters (Fig. 3*B*). In light of this, we used this projection of the linear filter on the first principal component to quantify the visual response kinetics. A projection of 0 represents the average filter shape, negative values represent filters with faster and more biphasic filters, while positive values are slower and monophasic. For the response of the GC to SOA current injection, we measured the duration of the firing burst as the time required to fire 80% of the spikes. Using these metrics, one finds indeed that the kinetics of the visual response and the response to SOA hyperpolarization are related. In particular, GCs with a slow visual response always had a sustained response to SOA current injection (Fig. 3*B*).
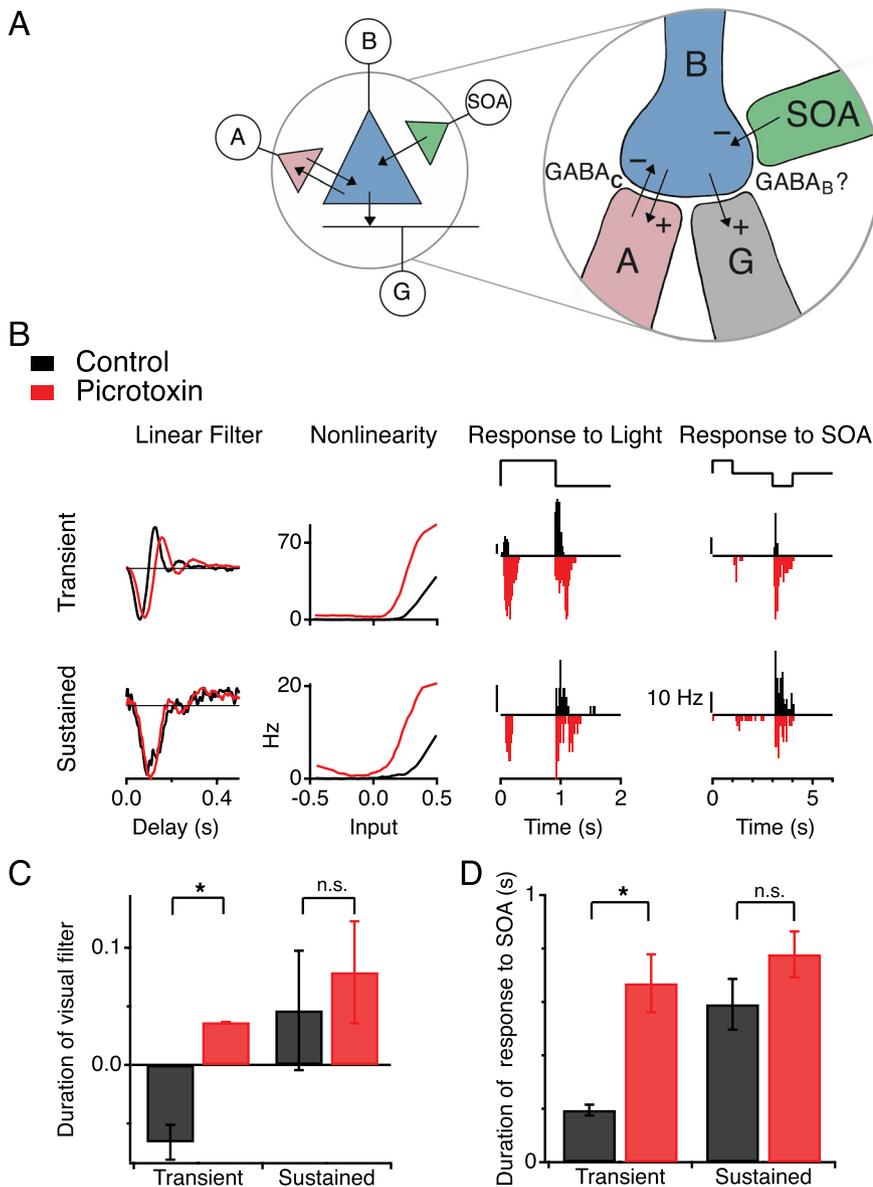
Figure 4. Block of GABA$_A$/GABA$_C$ transmission makes the effects of SOA stimulation more sustained. **A**, Schematic of proposed interactions at the bipolar cell synaptic terminal. B, Bipolar cell; A, other amacrine cell; G, ganglion cell; synapses are excitatory (+) or inhibitory (−). **B**, Responses to light and to SOA current injection of two sample ganglion cells (top, transient; bottom, sustained), with and without 200 μM picrotoxin in the bath. Left, LN model of the light response displayed as in Figure 1 D. Middle, Firing rate under uniform light steps (top stimulus trace); results in picrotoxin are plotted downward for easy comparison. Right, Firing rate under SOA current injection (top stimulus trace; ±0.5 nA); results in picrotoxin are plotted downward. **C**, Visual response kinetics for transient and sustained GCs, with and without 200 μM picrotoxin. The response duration is measured by the filter shape from the LN model as in Figure 3B, using the same principal components in both conditions. Large numbers mean sustained responses. *$p < 0.02$. **D**, Duration of response to SOA stimulation for transient and sustained GCs, with and without 200 μM picrotoxin. Response duration measured as in Figure 3B. *$p < 0.03$.

A GABA$_C$ circuit shapes the output of sustained OFF amacrine cells

This similarity between the response kinetics under light stimulation and SOA hyperpolarization suggests that a common mechanism shapes the responses of the GC to both stimuli. Although circuits in both outer and inner retina have been shown to shape GC visual responses, the above observations point to a mechanism in the inner retina that lies downstream of the sustained OFF amacrine cell. In particular, it has been proposed that the transient visual responses of certain GCs are enhanced by a reciprocal feedback circuit between bipolar and amacrine cells that

truncates the synaptic output of the bipolar cell after a brief delay (Nirenberg and Meister, 1997; Dong and Werblin, 1998). This feedback is thought to act via GABA$_C$ receptors on the terminals of the bipolar cells (Fig. 4A). To test this mechanism, we applied 200 μM picrotoxin, an antagonist at GABA$_A$ and GABA$_C$ receptors, and examined its effects on the kinetics of ganglion cell responses.

Picrotoxin prolonged the visual responses of transient GCs but did not affect the kinetics of the sustained GCs (Fig. 4B), consistent with previous reports (Zhang et al., 1997; Dong and Werblin, 1998). This is particularly clear on examination of the linear filters for these ganglion cells. In the presence of picrotoxin, the filter for the transient GCs broadened substantially (Fig. 4C). In addition, the nonlinearity for all GCs shifted strongly to the left (Fig. 4B), reflecting the general increase in excitability that results from blocking the action of GABA.

Just as picrotoxin prolonged the visual responses of transient GCs, it also prolonged the effects of SOA stimulation (Fig. 4B,D). Although these ganglion cells normally fired a brief burst of spikes at the onset of hyperpolarizing current into the SOA, in the presence of picrotoxin they fired throughout the duration of the pulse. The duration of the response to SOA hyperpolarization increased by a factor of 3.4 ± 0.2 for transient GCs but by only 1.4 ± 0.1 for sustained GCs (Fig. 4D). Because bicuculline, a GABA$_A$ receptor antagonist, did not alter the kinetics of GC responses to either stimulus (data not shown), we conclude that the effect of picrotoxin is attributable to its block of the GABA$_C$ receptor.

If the SOA acted primarily through direct inhibition of the GC, one would not expect this synaptic transmission to get stronger and slower in picrotoxin (Fig. 4B). Instead, we propose that the SOA acts presynaptically at the bipolar cell terminal, prior to a reciprocal feedback pathway that shapes the kinetics of transmission to the GC mediated by GABA (Fig. 4A). The feedback pathway involves GABA$_C$ receptors. In contrast, transmission from the SOA requires neither GABA$_A$ nor GABA$_C$ receptors, because it persists in picrotoxin. Strychnine, a glycine receptor blocker, likewise failed to eliminate the response of GCs to SOA stimulation (data not shown), so the SOA does not rely on glycine either.

GABA$_B$ receptors mediate tonic inhibition from sustained OFF amacrine cells

Although GABA$_A$ and GABA$_C$ are the predominant varieties of GABA receptors expressed in the retina, one also finds GABA$_B$

receptors on bipolar cell terminals (Maguire et al., 1989a). This metabotropic receptor couples to a variety of ion channels. To examine its role in the present effects, we repeated the experiments in 100 μM baclofen, a GABA$_B$ agonist. This dose is thought to saturate the GABA$_B$ receptors, leaving them insensitive to additional GABA release (Hare and Owen, 1996). In the presence of baclofen, the flash responses of sustained GCs became transient, whereas the responses of transient GCs were slightly enhanced (Fig. 5A), consistent with previous reports (Slaughter and Bai, 1989; Tian and Slaughter, 1994). However, the ganglion cell responses to SOA hyperpolarization were completely abolished (Fig. 5A,B). This suggests that the sustained OFF amacrine cell is GABAergic and acts via GABA$_B$ receptors.

An alternative interpretation is that, by saturating the GABA$_B$ receptors, baclofen effectively suppresses transmission from the bipolar cell terminal and thus obscures signaling from the SOA to the terminal regardless of what receptors are involved. Indeed, the excitability of ganglion cells declined in 100 μM baclofen: their firing rate under the random flicker stimulus fell by >75%, and the nonlinearity in the LN model shifted sharply rightward (Fig. 5A). However, ganglion cells still responded reliably to a uniform flash (Fig. 5A). Therefore, we took advantage of this stimulus to further explore the response to SOA stimulation. When the SOA was hyperpolarized coincident with light offset, this greatly increased the response of GCs compared with light offset alone (47 ± 19%) (Fig. 5C,D). In the presence of baclofen, however, this enhancement from SOA hyperpolarization was eliminated (2 ± 6%, p < 0.05). Thus, the effect of the SOA is blocked by a GABA$_B$ agonist even under conditions in which bipolar cells are clearly releasing glutamate onto ganglion cells.

The simplest explanation of the above effects is that the SOA tonically releases GABA, which acts on GABA$_B$ receptors at the bipolar terminal to suppress transmitter release. Hyperpolarization of the SOA reduces GABA release, relieves suppression of bipolar cell transmission, and thus enhances the light response. Baclofen extenuates the suppression through the same pathway.

Sustained OFF amacrine cells scale the visual sensitivity of ganglion cells

The ganglion cell responses to stimulation of the SOA offer a quick estimate of the projective field of the SOA. However, to understand the role of the amacrine cell in visual function, one needs to determine how its signals influence the visual responses of ganglion cells. As shown above, hyperpolarizing the SOA enhanced the GC response to light offset (Fig. 5C). To better examine these interactions, we presented a spatially uniform random flicker stimulus in combination with depolarizing or hyperpolar-
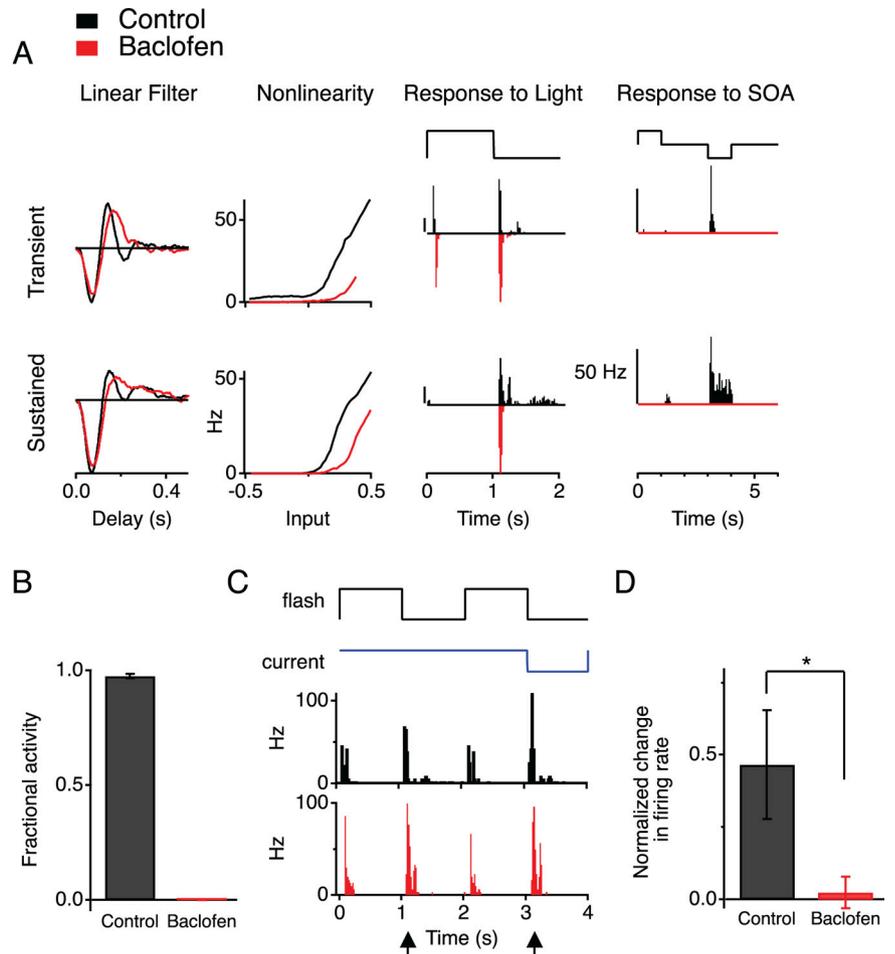

Figure 5. Block of GABA$_B$ transmission eliminates the effects of SOA stimulation. *A*, Responses to light and to SOA current injection of two sample ganglion cells (top, transient; bottom, sustained), with and without 100 μM baclofen in the bath. Display as in Figure 4B. *B*, Disinhibition of ganglion cells by SOA stimulation with and without 100 μM baclofen. Measured as the fraction of spikes that occur during the hyperpolarizing pulse into the SOA, as in Figure 2B. *C*, Firing rate of a ganglion cell stimulated by a combination of light flashes and SOA current, with and without 100 μM baclofen. Arrowheads indicate the response to light OFF; the second of these transitions was paired with 0.5 nA hyperpolarizing current (top traces). *D*, Fractional change in the number of spikes fired at light OFF when the amacrine cell is hyperpolarized (right arrow in *C*) from when the amacrine cell is unperturbed (left arrow in *C*) (*p < 0.05, Student's t test, n = 7).

izing current pulses into an SOA. Based on the results discussed above, one expects that current injection should manipulate the tonic inhibition exerted by the SOA on bipolar cells and thus modulate their transmitter release. Indeed, we found that the GC firing rate decreased during SOA depolarization and increased sharply during SOA hyperpolarization (Figs. 6A,B).

To understand the nature of these altered ganglion cell responses, we computed separate LN models for GC firing both during and after the SOA current pulse. SOA depolarization raised the threshold of the GC nonlinearity (Fig. 6A,C), whereas hyperpolarization lowered the threshold (Fig. 6B,D). Even when the firing rate was raised >10-fold (Fig. 6B), all the ganglion cell spikes were strictly driven by the visual stimulus: the nonlinearity shows no evidence of spontaneous firing (Fig. 6D). Furthermore, the shape of the GC filter function remained entirely unaffected (Fig. 6C,D). We conclude that SOA depolarization suppresses the sensitivity of the GC to visual stimuli. In contrast, the SOA does not modulate the kinetics of the GC visual response.

In a more direct examination, we compared spiking responses of a GC to the exact same stimulus sequence repeated with and
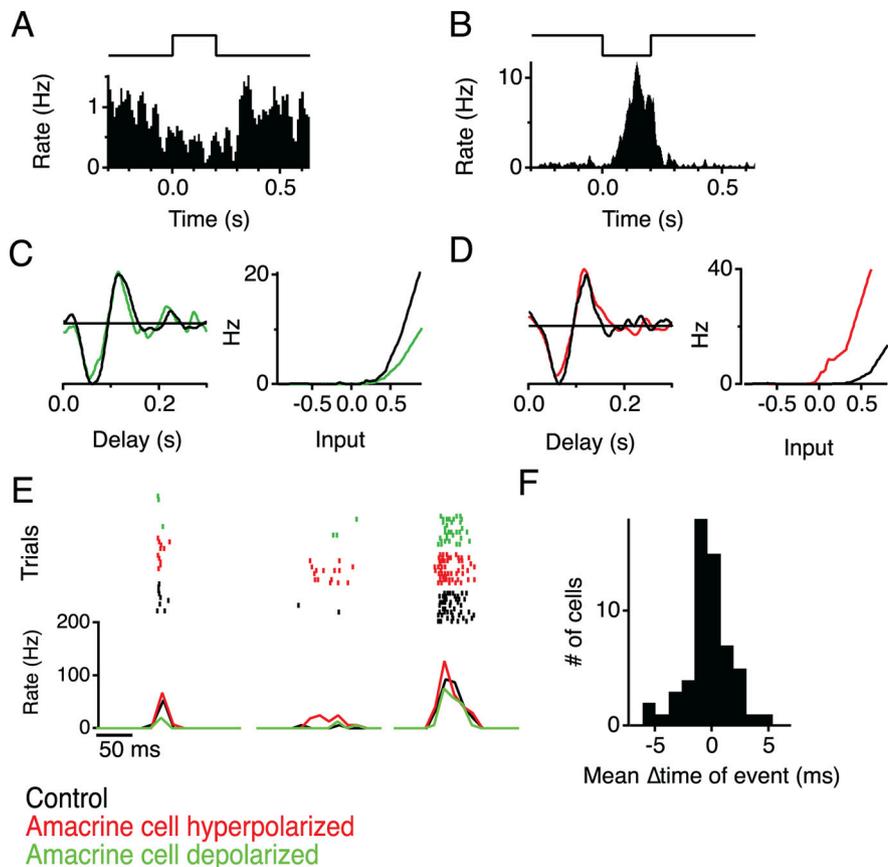
Figure 6. The sustained OFF amacrine cell modulates sensitivity but not kinetics of ganglion cell visual responses. ***A***, Firing rate of a ganglion cell triggered on a depolarizing current pulse delivered to the SOA (+1 nA, top trace). The stimulus consisted of uniform illumination whose intensity flickered with a pseudorandom waveform throughout. Current pulses occurred periodically every 1 s, independent of the light stimulus. ***B***, Firing rate of a ganglion cell (different from ***A***) triggered on a hyperpolarizing pulse to the SOA. ***C***, LN model of the ganglion cell visual response during and outside the depolarizing current pulse of ***A*** (color legend below ***E***). ***D***, LN model of the ganglion cell during and outside the hyperpolarizing current pulse of ***B***. ***E***, Ganglion cell firing events for the same random flicker stimulus sequence during SOA stimulation with +0.75, 0, and −0.75 nA. Top, Raster graph of repeated trials; bottom, average firing rate. To avoid effects of prolonged current injection, the three different conditions were interleaved. ***F***, Histogram of the average change in burst timing produced by SOA stimulation for 55 ganglion cells.

without SOA current injection. Corresponding bursts of spikes occurred at the same time under both conditions, but the number of spikes in the burst varied depending on current injection (Fig. 6 *E*,*F*). This confirms the conclusions drawn from the LN analysis: the SOA output affects the sensitivity of GCs to the stimulus but not the timing of their response.

Modeling

To summarize the interactions between the SOA and the visual responses of GCs, we tested whether we could capture all of the above results with a simplified cascade model of the amacrine and ganglion cell pathways (Fig. 7*A*). The direct pathway in this model represents signals that travel to the ganglion cell without SOA stimulation. It combines a monophasic filter for the outer retina, high-pass filtering through feedback at the bipolar cell terminal, and nonlinear transmission and spike generation at the ganglion cell. Its parameters were estimated from an LN fit to the GC response. In addition, a lateral pathway represents the effects of the SOA. Its properties are taken from the LN fit to the light response of the SOA. The two pathways were connected by an inhibitory multiplicative gain factor, such that SOA depolarization decreases the gain of the direct pathway.

The model produced brief increases in firing rate in response to a random flicker stimulus (Fig. 7*B*), as seen in real ganglion cell responses (Fig. 6 *E*). The effects of the SOA were summarized by calculating LN fits to the model GC response with and without the SOA pathway present. This altered the sensitivity of the ganglion cell, but its temporal filtering remained the same (Fig. 7*C*), just as observed in experiments (Fig. 6 *B*,*D*). These simulations show that the results of current injection and visual stimulation can be explained consistently by the same circuit model.

The projective field of sustained OFF amacrine cells has center-surround antagonism

Given that the SOA acts presynaptically at the bipolar cell terminal, its effects may not be uniform across the receptive field of a GC. To examine this, we used a flickering checkerboard stimulus to map the sensitivity within the spatiotemporal receptive field of a GC while injecting current into a SOA. Again the analysis was performed separately for periods during and outside of the current pulses. Depolarization of the SOA depressed the sensitivity of the GC but typically only in a small region of the receptive field (Fig. 8*A*). Other parts of the ganglion cell receptive field were unaffected or even experienced the opposite effect. This was observed for both ON and OFF ganglion cells (Fig. 8*B*). As a result, the output of the SOA altered the shape of nearby GC receptive fields.

We examined the overall effect of the SOA on the visual field, as represented across the ganglion cell population in an area ~1 mm in size (Fig. 9). By summing the effects of SOA depolarization over all recorded GCs, one finds that the decrease in sensitivity was restricted to only a small region, within ~100 μm of the SOA soma (Fig. 9*B*). The surrounding regions of the visual field actually experienced increased sensitivity. The fractional decrease in sensitivity in the center of the amacrine cell projective field was on average −0.1 ± 0.02 (n = 94 cell pairs), whereas the fractional increase in sensitivity in a given region of the projective field surround was 0.06 ± 0.01. Thus, the projective field of the SOA has a distinct center-surround organization, producing local inhibition and distant excitation (Fig. 9*B*,*C*).

Discussion

We have examined here the role of sustained OFF amacrine cells in the network of the salamander retina. These neurons have a small receptive field from photoreceptors but a much larger projective field onto ganglion cells (Figs. 1, 2). Hyperpolarization of just one of these amacrine cells is sufficient to elicit robust firing in nearby ganglion cells (Figs. 2–5). They tonically suppress the excitation of ganglion cells, most likely via presynaptic inhibition of bipolar cell terminals (Figs. 4, 5, 8). Under visual stimulation, this amacrine cell type modulates the visual sensitivity of gan-

glion cells but not their response kinetics (Figs. 6–8). In contrast, this amacrine cell does shape the spatial pattern of ganglion cell excitation, via the antagonistic center-surround effects it exerts on the output layer of the retina (Figs. 8, 9). Here we comment further on notable features of the projective field of this neuron.

Slow gain control

It is remarkable that tonic transmission from a single sustained OFF amacrine cell effects an average 10% suppression of all nearby ganglion cells (Fig. 9C) and in some cases much more (Fig. 6B). If the projective fields of several SOAs overlap in space, this cell type alone can account for a major modulation of ganglion cell sensitivity during visual stimulation. In contrast, the SOA does not appear to control the dynamics of the ganglion cell response. In general, amacrine cell circuits can emphasize the transients in bipolar cell signals, through feedforward and feedback inhibition (Maguire et al., 1989b; Nirenberg and Meister, 1997; Dong and Werblin, 1998; Roska et al., 1998). Indeed, we observed the action of these circuits when picrotoxin block of inhibition rendered ganglion cell responses more sustained (Fig. 4). However, the SOA was not involved in these effects. First, SOA transmission to GCs was resistant to picrotoxin. Second, SOA stimulation itself also produced more sustained effects under picrotoxin block, suggesting that it enters the bipolar cell before downstream circuits that produce the sharpening (Fig. 4A).

Another estimate of the temporal action of SOAs came from observing GC light responses during periods when the SOA was polarized by injected current. If the SOA were involved in the inhibitory circuits that sharpen response dynamics, one would expect such action to be altered somehow by extreme depolarization or hyperpolarization of the SOA. This did not occur, even though the effects on ganglion cell sensitivity were very pronounced (Figs. 6, 8). All these observations are consistent with a picture in which the SOA provides a slow and sustained inhibitory signal to the bipolar cell terminal. Under regular visual stimulation, this signal varies more slowly than the signals in bipolar cells and thus modulates the gain of the transmitter release of the bipolar cells in a gradual manner (Fig. 7).

Antagonistic spatial profile

The spatial extent of the receptive field and projective field of the SOA are consistent with its dendritic arborization. For example, the dendritic field of the SOA has a radius of ∼100 μm. Including the spatial reach of bipolar cell dendrites and terminals (Wu et al., 2000), this accounts for the ∼130 μm radius of the visual receptive field (Fig. 1). On the output side, one needs to include the radius of ganglion cell dendrites, up to ∼200 μm (Toris et al., 1995), which explains the ∼300 μm radius of the projective field of the SOA (Fig. 2). Many types of amacrine cells are coupled homotypically by gap junctions (Yang et al., 1991; Bloomfield
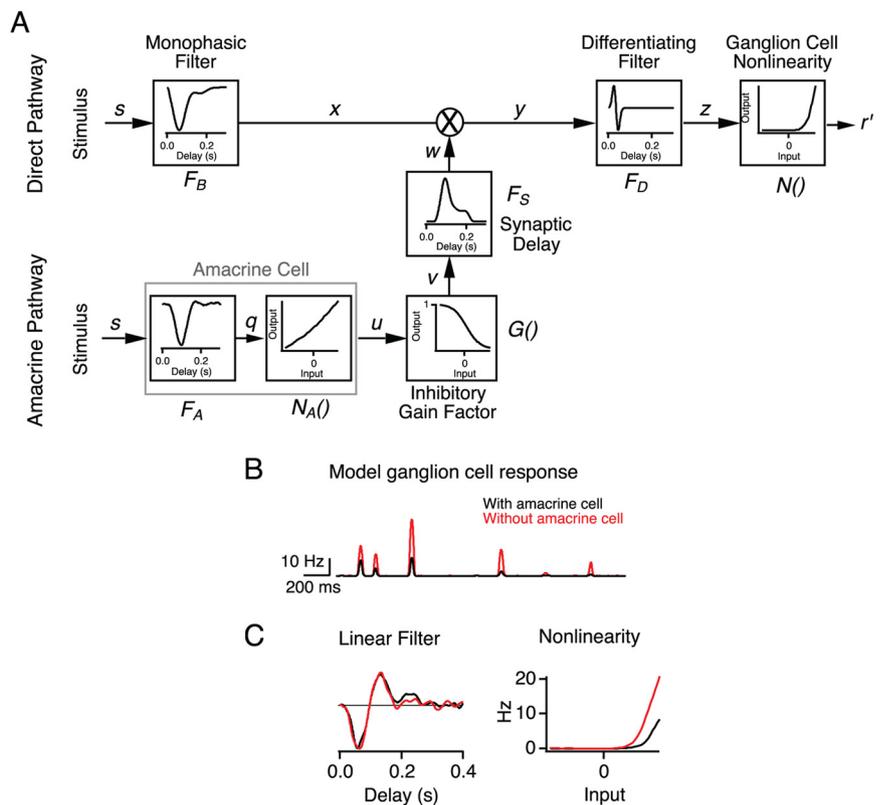

Figure 7. A cascade model that accounts for the receptive and projective fields of the SOA. **A**, Cascade model relating the visual stimulus (s), SOA signals (u), and GC firing (r′). The stimulus is spatially uniform as in Figures 3–6. The direct pathway (top) implements an LN model for the ganglion cell visual response. The lateral pathway (bottom) consists of an LN model of the SOA visual response, followed by inhibitory transmission that modulates the gain in the direct pathway of the GC. This model describes correctly the visual responses of the SOA and the GC, as well as the SOA effects on GC firing. For mathematical details, see Materials and Methods. **B**, Ganglion cell response of the model with the SOA pathway active or blocked; compare with Figure 6 E. **C**, LN model fit to the ganglion cell response with the SOA pathway active or blocked; compare to Figure 6 D.

and Xin, 1997); if this is the case for SOAs as well, it does not contribute substantially to the spatial extent of the receptive or the projective field.

Within that output region, however, the projective field has an antagonistic structure: the effect of the SOA changes from suppression to facilitation at ∼150 μm radius (Fig. 9). This antagonistic surround may be implemented by serial inhibition within the amacrine cell network (Roska et al., 1998; Marc and Liu, 2000) (Fig. 9D). Whether this lateral spread involves the same population of SOAs or a different cell type remains to be tested. In general, the amacrine cell network has been credited with implementing lateral inhibition among bipolar pathways, contributing to the antagonistic surround of the bipolar cell (Cook and McReynolds, 1998; Jacobs and Werblin, 1998; Ichinose and Lukasiewicz, 2005). By the same token, this network may shape the downstream effects of individual amacrine cells. In this respect, the amacrine cell network differs categorically from the horizontal cell network in the outer retina, which relies entirely on sign-preserving transmission among the interneurons.
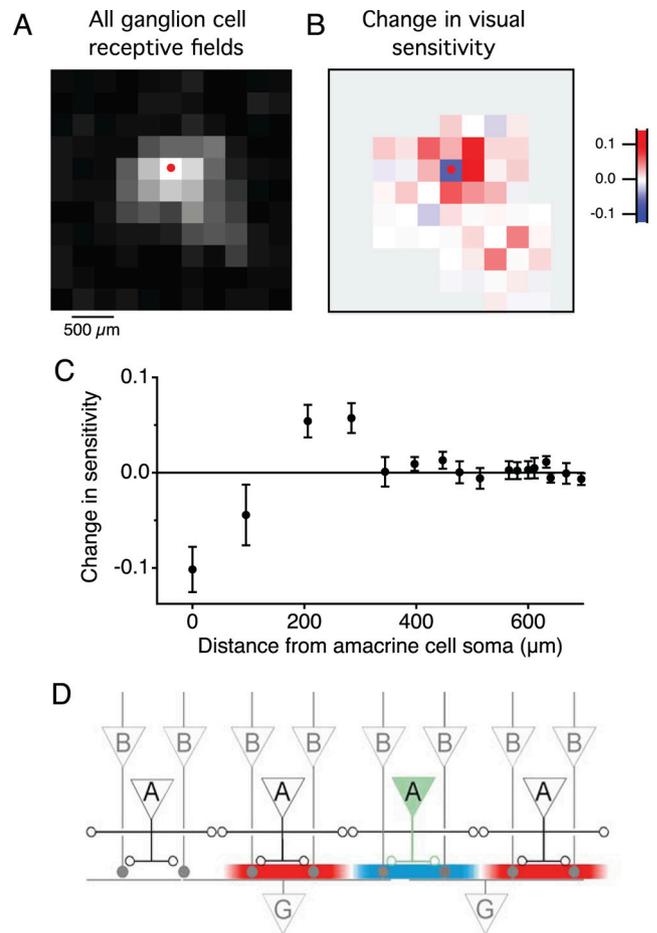
Predictive sensitization

What could be the purpose of this antagonistic processing in the inner retina? Any local event that excites the SOA will depress ganglion cell output locally but sensitize the retina in immediately neighboring regions. Because the SOA modulated the sensitivity of all ganglion cells in the same manner, regardless of polarity or kinetics, we see that this amacrine cell does not select
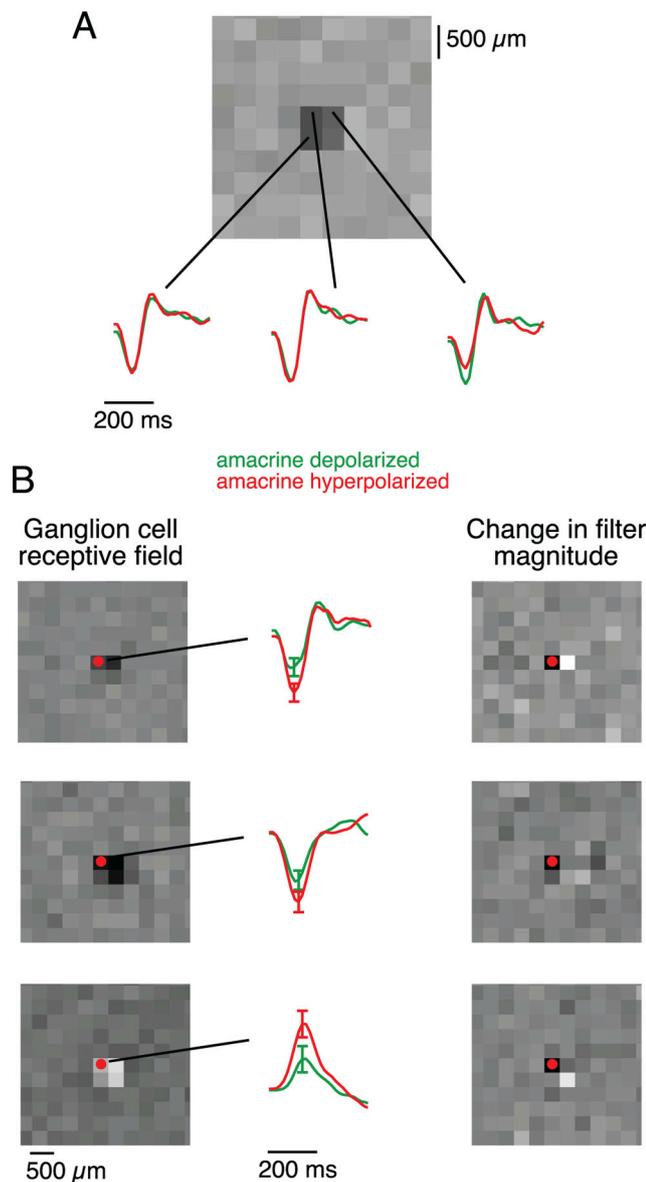
Figure 8. The SOA has differential effects within a ganglion cell receptive field. *A*, A ganglion cell spatiotemporal receptive field, illustrated with a spatial profile at the peak time (top) and time course in each indicated square (bottom). These were calculated separately when the SOA was depolarized or hyperpolarized. The amplitude of each waveform indicates sensitivity in that region. *B*, Receptive field changes induced by SOA stimulation in three sample ganglion cells (top to bottom). Left, Spatial receptive field. Dot indicates location of the amacrine cell soma. Middle, Time course of the receptive field at the location of the amacrine cell soma when the SOA was depolarized or hyperpolarized. Right, Change in visual sensitivity produced by SOA current injection. At each location, sensitivity was computed as the root-mean-square amplitude of the 300 ms time course (middle). Grayscale indicates the change in this sensitivity between the hyperpolarized and depolarized conditions. Note that the effect can have opposite sign in neighboring pixels.

Figure 9. The SOA projective field includes local suppression and lateral facilitation. *A*, Sum of visual sensitivity in the receptive field centers of 55 ganglion cells. For each GC, a sensitivity profile was computed as in Figure 8*B*. The graph shows the sum of those profiles. *B*, Change in visual sensitivity produced by SOA current injection, averaged across all ganglion cells. This plots the change in the profile of *A* between the conditions with the SOA depolarized and hyperpolarized. Dot indicates location of the amacrine cell soma. Pixels without significant receptive fields are shown in gray. *C*, Change in visual sensitivity for each square plotted against the distance between that square and the amacrine cell soma, for three amacrine cells and 94 ganglion cells. *D*, Circuit schematic to account for facilitatory and suppressive regions of the projective field. Filled/open circles are excitatory/inhibitory synapses. Depolarization of the shaded SOA leads to inhibition of local bipolar cell terminals and—via serial inhibition among amacrine cells—to disinhibition of more distant ones.

sion on the trailing side will produce a shift of the neural representation in the direction of motion (Berry et al., 1999), thus contributing to motion anticipation. More generally, one can regard the surround of the projective field of the SOA as sensitizing the retina based on the prediction of impending activity.

Conclusions

Inhibitory interneurons form a diverse population in many neural circuits—from sensory nuclei to cortical structures to motor areas—and they play a central role in gating and shaping the patterns of excitation. By definition, they are located somewhere in the middle of the circuit, and thus an understanding of their function must include both their receptive field to input signals and their projective field onto the outputs of the circuit. In making direct measurements of the projective field, we discovered aspects of retinal circuitry difficult to observe by other means, including the center-surround projective field of amacrine cells and the control of gain without modulation of kinetics. Certainly

specific visual features to enhance but serves to sensitize all visual coding in the vicinity. Those are the most likely places where the event will occur next, either from an eye movement of the observer or as a result of motion of an object within the scene.

It is instructive to think about the special case of a moving small object. The SOA circuits will enhance the gain of all ganglion cells ahead and behind the object location. Other mechanisms of gain control contribute a strong depression on the trailing side (Shapley and Victor, 1978; Kim and Rieke, 2003). Together, the gain enhancement on the leading side and depres-

the retina offers advantages for parallel recording of output signals, but the new opportunities afforded by optical tools for recording and stimulation should enable a broader effort to understand projective fields in other circuits of the brain. This would provide an essential complement to the ubiquitous studies of receptive fields.

References

Baccus SA (2007) Timing and computation in inner retinal circuitry. Annu Rev Physiol 69:271–290.

Baccus SA, Meister M (2002) Fast and slow contrast adaptation in retinal circuitry. Neuron 36:909–919.

Baccus SA, Olveczky BP, Manu M, Meister M (2008) A retinal circuit that computes object motion. J Neurosci 28:6807–6817.

Berry MJ 2nd, Brivanlou IH, Jordan TA, Meister M (1999) Anticipation of moving stimuli by the retina. Nature 398:334–338.

Bloomfield SA, Xin D (1997) A comparison of receptive-field and tracer-coupling size of amacrine and ganglion cells in the rabbit retina. Vis Neurosci 14:1153–1165.

Burkhardt DA, Fahey PK, Sikora M (1998) Responses of ganglion cells to contrast steps in the light-adapted retina of the tiger salamander. Vis Neurosci 15:219–229.

Chichilnisky EJ (2001) A simple white noise analysis of neuronal light responses. Network 12:199–213.

Cook PB, McReynolds JS (1998) Lateral inhibition in the inner retina is important for spatial tuning of ganglion cells. Nat Neurosci 1:714–719.

Dong CJ, Werblin FS (1998) Temporal contrast enhancement via $GABA_C$ feedback at bipolar terminals in the tiger salamander retina. J Neurophysiol 79:2171–2180.

Euler T, Detwiler PB, Denk W (2002) Directionally selective calcium signals in dendrites of starburst amacrine cells. Nature 418:845–852.

Field GD, Chichilnisky EJ (2007) Information processing in the primate retina: circuitry and coding. Annu Rev Neurosci 30:1–30.

Flores-Herr N, Protti DA, Wässle H (2001) Synaptic currents generating the inhibitory surround of ganglion cells in the mammalian retina. J Neurosci 21:4853–4863.

Gollisch T, Meister M (2010) Eye smarter than scientists believed: neural computations in circuits of the retina. Neuron 65:150–164.

Hare WA, Owen WG (1996) Receptive field of the retinal bipolar cell: a pharmacological study in the tiger salamander. J Neurophysiol 76:2005–2019.

He S, Masland RH (1997) Retinal direction selectivity after targeted laser ablation of starburst amacrine cells. Nature 389:378–382.

Ichinose T, Lukasiewicz PD (2005) Inner and outer retinal pathways both contribute to surround inhibition of salamander ganglion cells. J Physiol 565:517–535.

Jacobs AL, Werblin FS (1998) Spatiotemporal patterns at the retinal output. J Neurophysiol 80:447–451.

Jacoby R, Stafford D, Kouyama N, Marshak D (1996) Synaptic inputs to ON parasol ganglion cells in the primate retina. J Neurosci 16:8041–8056.

Kim KJ, Rieke F (2003) Slow Na^+ inactivation and variance adaptation in salamander retinal ganglion cells. J Neurosci 23:1506–1516.

Lehky SR, Sejnowski TJ (1988) Network model of shape-from-shading: neural function arises from both receptive and projective fields. Nature 333:452–454.

Maguire G, Maple B, Lukasiewicz P, Werblin F (1989a) Gamma-aminobutyrate type B receptor modulation of L-type calcium channel current at bipolar cell terminals in the retina of the tiger salamander. Proc Natl Acad Sci U S A 86:10144–10147.

Maguire G, Lukasiewicz P, Werblin F (1989b) Amacrine cell interactions underlying the response to change in the tiger salamander retina. J Neurosci 9:726–735.

Marc RE, Liu W (2000) Fundamental GABAergic amacrine cell circuitries in the retina: nested feedback, concatenated inhibition, and axosomatic synapses. J Comp Neurol 425:560–582.

Masland RH (1999) Amacrine cells: morphology, physiology and transmitters. In: The retinal basis of vision (Toyoda J, Murakami M, Kaneko A, Saito T, eds), pp 125–139. Amsterdam: Elsevier Science.

Masland RH (2001) The fundamental plan of the retina. Nat Neurosci 4:877–886.

Meister M, Pine J, Baylor DA (1994) Multi-neuronal signals from the retina: acquisition and analysis. J Neurosci Methods 51:95–106.

Münch TA, da Silveira RA, Siegert S, Viney TJ, Awatramani GB, Roska B (2009) Approach sensitivity in the retina processed by a multifunctional neural circuit. Nat Neurosci 12:1308–1316.

Nirenberg S, Meister M (1997) The light response of retinal ganglion cells is truncated by a displaced amacrine circuit. Neuron 18:637–650.

Olveczky BP, Baccus SA, Meister M (2003) Segregation of object and background motion in the retina. Nature 423:401–408.

Pang JJ, Gao F, Wu SM (2002) Relative contributions of bipolar cell and amacrine cell inputs to light responses of ON, OFF and ON-OFF retinal ganglion cells. Vision Res 42:19–27.

Roska B, Nemeth E, Werblin FS (1998) Response to change is facilitated by a three-neuron disinhibitory pathway in the tiger salamander retina. J Neurosci 18:3451–3459.

Segev R, Puchalla J, Berry MJ 2nd (2006) Functional organization of ganglion cells in the salamander retina. J Neurophysiol 95:2277–2292.

Shapley RM, Victor JD (1978) The effect of contrast on the transfer properties of cat retinal ganglion cells. J Physiol 285:275–298.

Slaughter MM, Bai SH (1989) Differential effects of baclofen on sustained and transient cells in the mudpuppy retina. J Neurophysiol 61:374–381.

Tachibana M, Kaneko A (1988) Retinal bipolar cells receive negative feedback input from GABAergic amacrine cells. Vis Neurosci 1:297–305.

Taylor WR (1999) TTX attenuates surround inhibition in rabbit retinal ganglion cells. Vis Neurosci 16:285–290.

Tian N, Slaughter MM (1994) Pharmacology of the GABA-B receptor in amphibian retina. Brain Res 660:267–274.

Toris CB, Eiesland JL, Miller RF (1995) Morphology of ganglion cells in the neotenous tiger salamander retina. J Comp Neurol 352:535–559.

Wässle H (2004) Parallel processing in the mammalian retina. Nat Rev Neurosci 5:1–11.

Wässle H, Boycott BB (1991) Functional architecture of the mammalian retina. Physiol Rev 71:447–480.

Werblin FS, Copenhagen DR (1974) Control of retinal sensitivity III. Lateral interactions at the inner plexiform layer. J Gen Physiol 63:88–110.

Wu SM, Gao F, Maple BR (2000) Functional architecture of synapses in the inner retina: segregation of visual signals by stratification of bipolar cell axon terminals. J Neurosci 20:4462–4470.

Yang CY, Lukasiewicz P, Maguire G, Werblin FS, Yazulla S (1991) Amacrine cells in the tiger salamander retina: morphology, physiology, and neurotransmitter identification. J Comp Neurol 312:19–32.

Zhang AJ, Wu SM (2010) Responses and receptive fields of amacrine cells and ganglion cells in the salamander retina. Vision Res 50:614–622.

Zhang J, Jung CS, Slaughter MM (1997) Serial inhibitory synapses in retina. Vis Neurosci 14:553–563.

Zhou ZJ, Lee S (2008) Synaptic physiology of direction selectivity in the retina. J Physiol 586:4371–4376.